Purinergic Signalling (2026) 22:9
https://doi.org/10.1007/s11302-025-10127-1

RESEARCH

Abnormal purinergic signaling contributes to development of renal cysts in autosomal dominant polycystic kidney disease

Veniamin Ivanov[1,2] · Andrew Wu[1,2] · Letizia Crocetti[3] · Ze Meng[4] · Puja Shrestha-Maskey[1] · Tang-Dong Liao[1] · Indra Adrianto[4,5] · Gabriella Guerrini[3] · Pablo A. Ortiz[1,2] · Tengis S. Pavlov[1,2]

Received: 29 May 2025 / Accepted: 9 October 2025 / Published online: 20 January 2026

Abstract

Polycystic kidney diseases (PKD) are a group of inherited nephropathies marked by the formation of fluid-filled cysts along the nephron, which cause renal failure. Bulk RNA sequencing of microdissected renal cysts from $Pkd1^{RC/RC}$ mice identifies 4,970 differentially expressed genes in comparison to intact collecting ducts. A poorly understood factor of cyst growth is the high ATP level in the cyst fluid, probably released by pannexin-1 hemichannels. Here, we evaluate a novel pannexin-1 inhibitor SIL14 as a potential therapeutic agent for cyst reduction and investigate proteins involved in cystogenesis, with a focus on purinergic signaling. In patch-clamp experiments, acute SIL14 application demonstrated strong, dose-dependent inhibition of Pannexin-1-dependent currents ($IC_{50} = 12.96$ μM). Chronic treatment of renal collecting duct cells with 30 μM SIL14 significantly reduced cyst size in a Matrigel model of cyst formation. Notably, RNA sequencing reveals that purinergic receptors P2Y2 and P2Y4, normally expressed in collecting ducts, were downregulated, while P2X5, P2X7, P2Y6, and P2Y12 were upregulated in the cystic epithelium. Stimulation with α,βMe-ATP or Bz-ATP (P2X7 agonists) increased cyst size and pannexin-1 expression in Matrigel cultures. Our findings indicate that the transition of normal collecting ducts to cystic epithelium is accompanied by distorted purinergic signaling and propose inhibition of luminal ATP release via pannexin-1 is a potential method to limit cystogenesis.

Keywords Purinergic signaling · Polycystic kidney diseases · ATP · Pannexin

Introduction

Polycystic kidney diseases belong to a group of inherited disorders characterized by the development of multiple cysts of epithelial origin, which cause renal failure and need in organ transplantation. Most of the autosomal dominant PKD cases are due to mutations in the structure of *PKD1* or *PKD2* genes and manifest in adults [1]. The autosomal recessive form of PKD is more aggressive [2], often found in the pre- or perinatal period, and caused by a mutation in *PKHD1*. Extrarenal manifestations may include hepatic cysts, aneurysm, and bile duct obstruction.

Renal cyst growth is a complex process in which normal epithelium of the nephrons (structural units of the kidney) starts uncontrolled proliferation, dilation, and loss of structure. Consistently across transcriptomic studies, PI3K/Akt, Hippo, small G proteins, inflammatory, metabolic, and oncogenic pathways underlie the disruptions caused by polycystin-1 deficiency [3–7]. One poorly understood aspect of this transition is distorted purinergic signaling. In regular physiology, extracellular ATP is one of many paracrine factors regulating cell functions such as transport across epithelia. In the distal nephron, abundant P2Y2 and P2Y4 receptors limit sodium reabsorption in case of excess dietary salt consumption [8, 9]. Both in ADPKD and ARPKD, the distal

✉ Tengis S. Pavlov
Tpavlov1@hfhs.org

1 Division of Hypertension and Vascular Research, Department of Medicine, Henry Ford Health, 6135 Woodward Ave, Detroit, MI 48202, USA

2 Department of Physiology, Wayne State University, 6135 Woodward Ave, Detroit, MI 48202, USA

3 Department of Neurofarba, Pharmaceutical and Nutraceutical Section, University of Florence, Via Ugo Schiff 6, 50019 Sesto Fiorentino, Italy

4 Department of Public Health Sciences, Henry Ford Health, 1 Ford Pl, Detroit, MI 48202, USA

5 Department of Medicine, College of Human Medicine, Michigan State University, East Lansing, MI 48824, USA

segments of the nephron, collecting ducts, develop ~ 70–80% of the cysts [10]. As shown in patients and animal models [11], cyst fluid contains a high level of ATP, which affects the distribution of purinergic receptors [12]. Earlier, we found a shift towards the prevalence of P2X and a reduction of P2Y receptors in ARPKD cystic epithelium [12].

The source of ATP in the cysts remains largely unknown. Recently we found high expression of pannexin-1, an ion channel permeable for ATP, in the ADPKD patient biopsies and cyst walls of $Pkd1^{RC/RC}$ mice, a model of ADPKD [13, 14]. We also administered *in-vivo* probenecid, a non-specific blocker of pannexin-1 and anion transporters, and found a beneficial effect against cyst development in this model. Here, we test a new and selective pannexin-1 channel blocker with a quinoline structure, named SIL14 (described as **6 g** in [15]), as a potential treatment against cyst development and identify proteins potentially involved in cystogenesis, with special interest in purinergic signaling.

Methods

Animals Mayo Clinic provided $Pkd1^{RC/RC}$ mice [16], for breeding at the Henry Ford Health System. Twenty-two-month-old females were aged in standard housing conditions and used for specimen collection under Wayne State University IACUC protocol according to ARRIVE guidelines. The $Pkd1^{RC/RC}$ mouse strain carries the human ADPKD p.R3277C allele introduced as *Pkd1* c.9805.9807AGA > TGC modification to the C57Bl/6N background. The strain is a hypomorphic model of ADPKD with development of multiple cysts in adult and mature animals.

RNA sequencing Collecting ducts and cystic epithelia were isolated from the kidneys of the same animals by microdissection with sharp forceps under stereomicroscope similarly to earlier publications [17, 18]. Bulk RNA was isolated and Qubit RNA High Sensitivity kit (Thermo Fisher Q32852) was used to quantify RNA. Full-coverage transcriptomes were obtained by RNAseq using an Ion Torrent Gene Studio Platform (Thermo Fisher) with quantifications of 16 000 to 19 000 mRNA transcripts per sample. Similarly to our earlier approach [19], analysis of differentially expressed genes between the cysts and collecting ducts was conducted using a negative binomial generalized linear model as implemented in the DESeq2 R/Bioconductor package. The data were normalized using the DESeq2 normalization method where the raw counts were divided by sample-specific size factors calculated by the median ratio of gene counts relative to the geometric mean per gene. All genes with an absolute log2 fold change > 1, base mean counts > 10 and false discovery rate (FDR) or q-value < 0.05 were subsequently promoted for biological pathway analysis using the Ingenuity Pathway Analysis (IPA) software (Qiagen Inc.). Additionally, differentially expressed genes were filtered using pathway-specific and disease-associated genes obtained from online consortiums and genome-wide association studies. Genes associated with ADPKD and CKD were obtained from the Online Mendelian Inheritance in Man database [20] and GWAS Catalog [21], respectively. Ciliary genes were obtained from the CiliaCarta database [22]. The purinergic signaling reference list of genes was obtained from Wikipathways [23] and the Mouse Genome Informatics database [24, 25]. Visualization of the differentially expressed genes was created using Cytoscape [26].

Epithelial cell culture The $mpkCCD_{cl4}$ cell line, representing epithelial cells of mouse cortical collecting ducts, was previously characterized and extensively employed in the studies, focused on sodium and water transport [27, 28]. Key experiments were reproduced in canine renal epithelial MDCK cells (ATCC CCL-34). Cells were grown in DMEM:F12 media (10–090-CV), containing 2% FBS, 1% insulin-transferrin-selenium mix (Gibco 41,400–045), and 1% Penicillin–Streptomycin Glutamine (Gibco 10,378–016). $MpkCCD_{cl4}$ and MDCK cells were used to model cyst development in 3D culture similarly to Mangoo-Karim and colleagues [29]. Approximately 5,000 cells were mixed 1:1 in Matrigel (Corning 356,234), passaged with 10 µM forskolin (Tocris 1099), and vehicle/SIL14/α,βMe-ATP/BzATP were added in wells (24 well plate Corning 3598). Cysts were grown for three weeks ($mpkCCD_{cl4}$) or one week (MDCK), calibrated images were acquired with an Olympus IX81 inverted microscope interfaced via Metamorph software, and sizes of the cysts were measured with Fiji software package (NIH) by manual selection of each cyst wall borders. Cysts also were washed, fixed in 2% paraformaldehyde, permeabilized for 1 h in 0.2% Triton X-100, blocked with 3% BSA for 1 h, and stained for pannexin-1 and F-actin visualization under a Leica multi-photon microscope (Alomone ACC-234 [30] and Thermo Scientific A11011 antibodies, FITC-phalloidin F432).

Patch-clamp electrophysiology CHO-K1 cells (CCL-61, ATCC) were grown, transfected, and prepared for patch-clamp as reported earlier [31]. Briefly, 0.5 µg mPanx1 and 0.5 µg mGFP cDNA plasmids were transfected into the cells, seeded onto glass chips with Lipofectamine 3000 (#MR206795, #TR30007, Origene, and #L3000-008, Invitrogen). One to three days later, currents were acquired and subsequently analyzed with an Axopatch 200B amplifier (Axon Instruments, CA, USA) and Bessel filter LPF-8 at 200 kHz (Warner Instruments, CT, USA), interfaced via a Digidata 1550B to a PC running the pClamp 10.6 suite of software (Axon Instruments, CA, USA). For each patch-clamp

experiment, a glass chip with cells was transferred into the chamber with a constant flow of bath solution, placed under the inverted microscope Nikon Ti-S. Whole-cell macroscopic current recordings of pannexin-1 were made under voltage-clamp conditions with ramp protocol (90- > −90 mV). The pipette solution contained (in mM): 120 $CsCl_2$, 5 NaCl, 2 $MgCl_2$, 5 EGTA, 2 Mg-ATP, 0.1 GTP, and 10 mM HEPES (pH 7.4); extracellular solution 140 mM NaCl, 3 mM KCl, 2 mM $MgCl_2$, 2 mM $CaCl_2$, and 10 mM HEPES (pH 7.4).

In situ hybridization Formalin-fixed *Pkd1*$^{RC/RC}$ mouse kidneys were cut in standard 4 µm histological slides, and *P2rx4* and *P2rx7* mRNA were detected with RNAScope® probes 21307 A and 23083B according to the manufacturer's recommendations (Advanced Cell Diagnostics). Slides were scanned on a Leica Histological Scanner at 40×, and signal intensity was quantified as the number of punctae per 100 µm of epithelial wall. Identification of proximal tubules and collecting ducts was based on lectin staining with Lotus Tetragonolobus (TLA) and Dolichos Biflorus (DBA) Agglutinins [16] (1:250 and 1:100 overnight at 4 °C).

Western blotting and rt-PCR MpkCCD$_{cl4}$ cysts were isolated from Matrigel using cell recovery solution (Corning 354,253) and lysed in cell extraction buffer (Invitrogen FNN0011) with Protease and Phosphatase inhibitors (Thermo Scientific 78,442). Samples were subjected to PAGE, transferred onto a PVDF membrane (Invitrogen LC2002), exposed to primary (Alomone ACC-234; APR-004) and HRP-conjugated secondary (Santa Cruz sc-2357) antibodies. The reaction was developed with an ECL (Thermo Scientific 34095). The band intensity was quantified by image analysis using Image J software. mRNA extraction from dissected kidney was performed using RNeasy Mini Kit (Qiagen 74104). cDNA was synthesized using 1 µg of RNA and iScript™ cDNA Synthesis Kit (Bio-Rad Cat. 1708890) according to manufacturer's protocol. cDNA and specific primers were mixed with iTaq Universal SYBR (Bio-Rad Cat. 1725121), and PCR reactions were run on a QuantStudio 7. Fold change in expression of target genes compared with the control was calculated using the $2-\Delta\Delta CT$ method with GAPDH. The sequences of the primers are shown in Supplementary Table 3.

Statistics Grubb's test was used to identify outliers. Data are presented as mean ± SEM. Normal distribution was confirmed with the Shapiro–Wilk test, and groups were compared with a *t*-test or ANOVA with correction for multiple comparisons (Dunnett tests). The nonlinear regression package in GraphPad Prism was used to determine IC_{50} in patch-clamp experiments.

Results

Massive alteration of transcriptome in cystic epithelia follows transition from normal collecting ducts To assess the expression profile of cystic epithelia, we performed bulk RNA sequencing, comparing intact collecting ducts and cysts, microdissected from mature C57BL/6 Pkd1$^{RC/RC}$ mouse (Fig. 1A). Our approach was based on that Pkd1$^{RC/RC}$ mouse cysts originate mostly from collecting ducts [32]. We identified 4970 differentially expressed genes after filtering (q-value < 0.05, |log2FC| > 1, base-mean > 10) (Fig. 1B) with PCA plot variance (Supplementary Fig. 1A). To understand the pathways associated with cystogenesis, we performed clustering of differentially expressed genes using our database of pathway-specific and disease-associated genes built from online consortiums and genome-wide association studies [20, 21, 33, 34] (Fig. 1C) and Interpretative Phenomenological Analysis (IPA) analysis (Supplementary Fig. 1B, Supplementary Table 2). Many of the pathways were previously reported to contribute to cystogenesis in ADPKD [35–39], including oncogenes, signs of chronic inflammatory responses (MSP-RON), and effect on cytoskeleton. Observed upregulated pathways, indeed, are interconnected: for example, small G-protein signaling upregulation together with RhoGDI inhibition suggests a regulatory interplay of Rho and Rac [40, 41] and can promote actin cytoskeleton rearrangement [41], epithelial-to-mesenchymal transition [42], fibrosis [43] and ERK/MAPK [44, 45] signaling.

We also filtered differentially expressed genes using specific signaling pathways and disease-associated genes obtained from online databases to validate the sensitivity of transcriptomics. As expected, hypomorphic *Pkd1* mutation decreased *Pkd1* expression, followed up with the downregulation of *Pkd2*. Notably, we observed a differential expression of genes, previously reported to be dependent on *Pkd1* and *Pkd2* by RNA-sequencing, such as Pank1, Gal3st1, Sh3gl2, Blk, and others [7]. Pank1 is a key enzyme in coenzyme A biosynthesis, indicating metabolic effects of cystic cell physiology, whereas Gal3st1, Sh3gl2, and Blk are oncogenes. Thus, the downregulation of *Adcy5* may be a compensatory reaction to cyst expansion because earlier Wang et al. and Hwang et al. reported the involvement of adenylyl cyclase 5 in cystogenesis. cAMP production in cilia is dependent on this enzyme, and *Adcy5* knockout mice have a rescued ADPKD phenotype [46, 47].

Development of cysts is accompanied by a shift in purinergic signaling We were able to identify clusters that we are particularly interested in, such as genes associated with chronic kidney disease and PKD. Interestingly, we also distinguished a purinergic signaling cluster. We observed a significant downregulation of purinergic receptors, normally

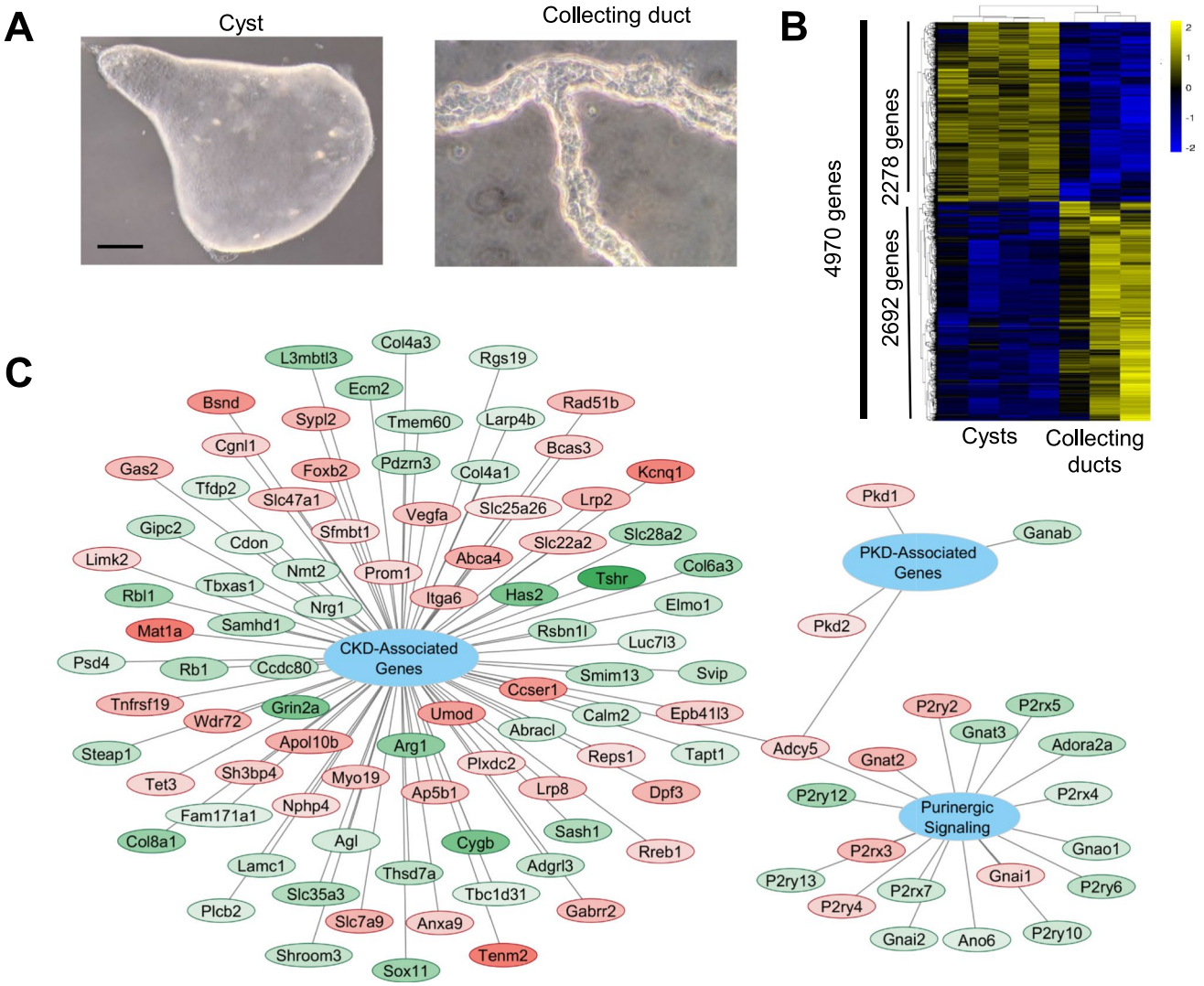

Fig. 1 RNA sequencing reveals massive change in the collecting ducts transcriptome due to transition to cystic epithelium. **A** Representative images of microdissected cysts and collecting ducts isolated from $Pkd1^{RC/RC}$ mice and analyzed with RNAseq. **B** Heatmap, showing mRNA expression of 4970 differentially expressed genes in cysts ($n=4$) vs. collecting ducts ($n=3$). **C** Clustering of the differentially expressed genes related to chronic kidney diseases, PKD, and purinergic signaling genes. Both the color and color intensity denote level of up- and downregulation in cysts. Scale bar 50 µm

expressed in collecting ducts [48]—P2Y2 and P2Y4—with a shift in prevalence towards P2X5, P2X7, P2Y6, and P2Y12 (Table 1).

The abundance of P2X receptors in the cysts is especially interesting because their interaction with pannexin-1 is well described as a stimulatory factor of ATP release [49, 50]. We used conventional rt-PCR to confirm upregulation of *P2rx7* expression in microdissected $Pkd1^{RC/RC}$ cysts versus normal cortical lysate from C57Bl/6 mice. Figure 2 demonstrates that various isoforms of *P2rx7* are more abundant in cystic epithelia than normal tissues.

In-situ hybridization is another technique confirming abnormal expression of *P2rx7* in cysts. We compared it with the abundance of *P2rx4*, which is not detected as

Table 1 Differential expression of purinergic receptors due to cyst growth

Gene	Log2 × change	*p*-value
Downregulated		
P2ry2	−2.25432	1.77×10^{-4}
P2ry4	−1.36698	8.04×10^{-3}
Upregulated		
P2rx5	2.884524	3.54×10^{-3}
P2rx7	1.52724	1.47×10^{-5}
P2ry12	3.136299	2.82×10^{-7}
P2ry6	2.141647	1.72×10^{-8}

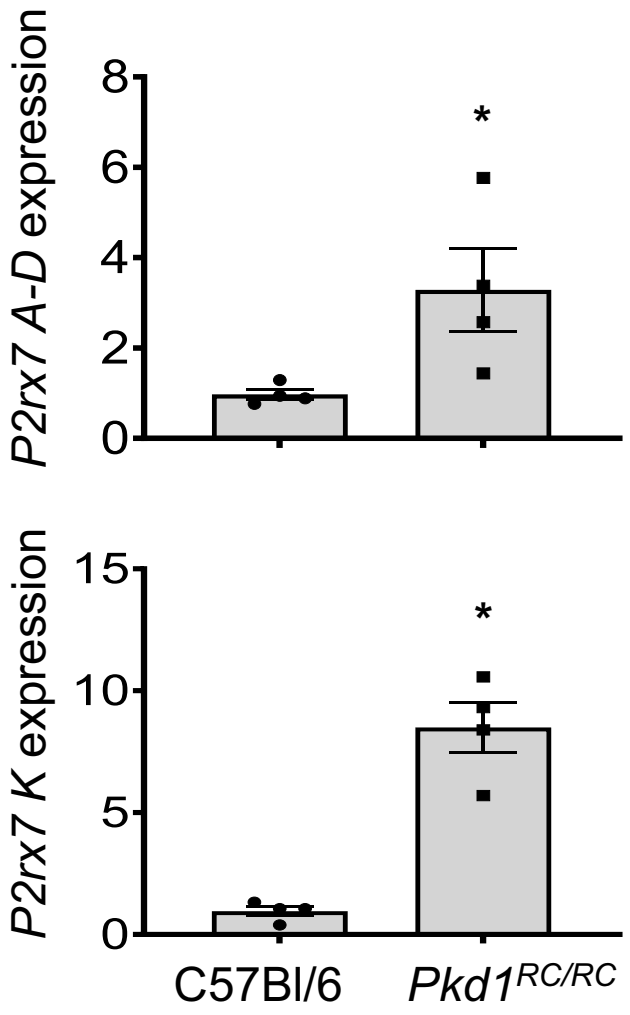

Fig. 2 *P2rx7* isoforms expression in normal C57Bl/6 vs *Pkd1*$^{RC/RC}$ mouse kidneys. Summary graph of real-time PCR measures *P2rx7 A-D* isoforms and *P2rx7 K* mRNA abundance in kidney cortex relative to GAPDH ($n=4$ mice) *$p<0.05$ Shapiro–Wilk (passed) and unpaired *t*-test

differentially expressed by RNAseq but also is suggested to interact with pannexin-1 in tumor or immune cells. Figure 3 demonstrates RNAscope staining against both P2X receptors' mRNA in two consecutive slices of a *Pkd1*$^{RC/RC}$ mouse kidney. *P2rx4* mRNA signal is abundant in all epithelial structures, especially in proximal tubules, with a lower but sufficient level both in collecting ducts and cysts. In contrast, *P2rx7* signal is not abundant in healthy epithelia, but cyst walls and pericystic space have expression of *P2rx7* mRNA. In healthy tissues, consistent *P2rx7* signal is detectable only in intratubular space, probably indicating immune or cell infiltration. Identification of proximal tubules and collecting ducts' morphology was facilitated by specific labeling with lectins Lotus Tetragonolobus (LTA) and Dolichos Biflorus (DBA) agglutinins (Supplementary Fig. 2). Similarly to earlier reports [16, 51], LTA labeling is abundant in the brush border of proximal tubules, whereas collecting ducts and cysts are DBA-reactive.

P2X7 interaction with pannexin-1 stimulates cystogenesis We hypothesized that the contribution of pannexin-1 activity to cyst growth can be exacerbated by the specific P2X7 overexpression in the mouse cysts. The *P2rx7* mRNA abundance data are in accordance with our earlier immunohistochemical findings [14] that cysts have abnormally high P2X7 protein levels. Here we tested how stimulation of P2X receptors affects cystogenesis in Matrigel. Figures 4A–-B demonstrate that culturing mpkCCD$_{cl4}$ cells in the presence of 50 μM α,βMe-ATP increases the size of formed cysts. In the end of the experiment, the cysts were collected and subjected to Western blotting. Stimulation of P2X increases pannexin-1 abundance (Fig. 4C) in the cysts.

To confirm these data, we used another cell culture – canine MDCK cells and performed experiments in the same conditions. In addition to α,βMe-ATP, a non-selective P2X agonist, we tested Bz-ATP, a P2X7 agonist, which could not be used on mpkCCD$_{cl4}$ cells due to low affinity to mouse P2X7. Figure 4D shows that MDCK cells in Matrigel form cell agglomerates (left panel) but in the presence of forskolin they develop into cysts significantly larger than mpkCCD$_{cl4}$ cysts (right panel). Both agonists increased cysts' size (Fig. 4E) and expression of pannexin-1 (Fig. 4F). We tested if an increased pannexin-1 abundance occurs also in the cysts isolated from *Pkd1*$^{RC/RC}$ mice and confirmed a higher expression in comparison to normal tubules of wild-type c57Bl/6 mice (Fig. 5). We concluded that pannexin-1 can serve as a target in ADPKD drug discovery.

SIL14 inhibits pannexin-1 activity We tested (Fig. 6A, B, C, D) a novel pharmacological agent, SIL14 (Fig. 5A), as a pannexin-1 blocker. Purinergic signaling differs in cold- and warm-blooded species, and although the inhibitory properties of SIL14 against *mPanx1* product were tested using a two-electrode voltage clamp [15] on *X. laevis* cells, we confirmed its effect on the mammalian heterologous system. Mouse pannexin-1 was reconstituted in hamster ovarian cells, and whole-cell currents elicited under voltage-clamp conditions. Similarly to earlier publications [31, 52], pannexin-1 demonstrates outward rectifying properties, and CHO cells develop a current density of 205 ± 24 pA/pF at +80 mV (Fig. 5B, C). Application of SIL14 rapidly inhibits current with $IC_{50} = 12.96$ μM (Fig. 5D).

SIL14 precludes growth of cysts formed by renal epithelial cells MpkCCD$_{cl4}$ and MDCK cells represent cortical collecting duct primary cells, with the ability to form polar monolayers, tight junctions, ENaC-dependent sodium reabsorption, and AQP2-mediated water permeability. In the

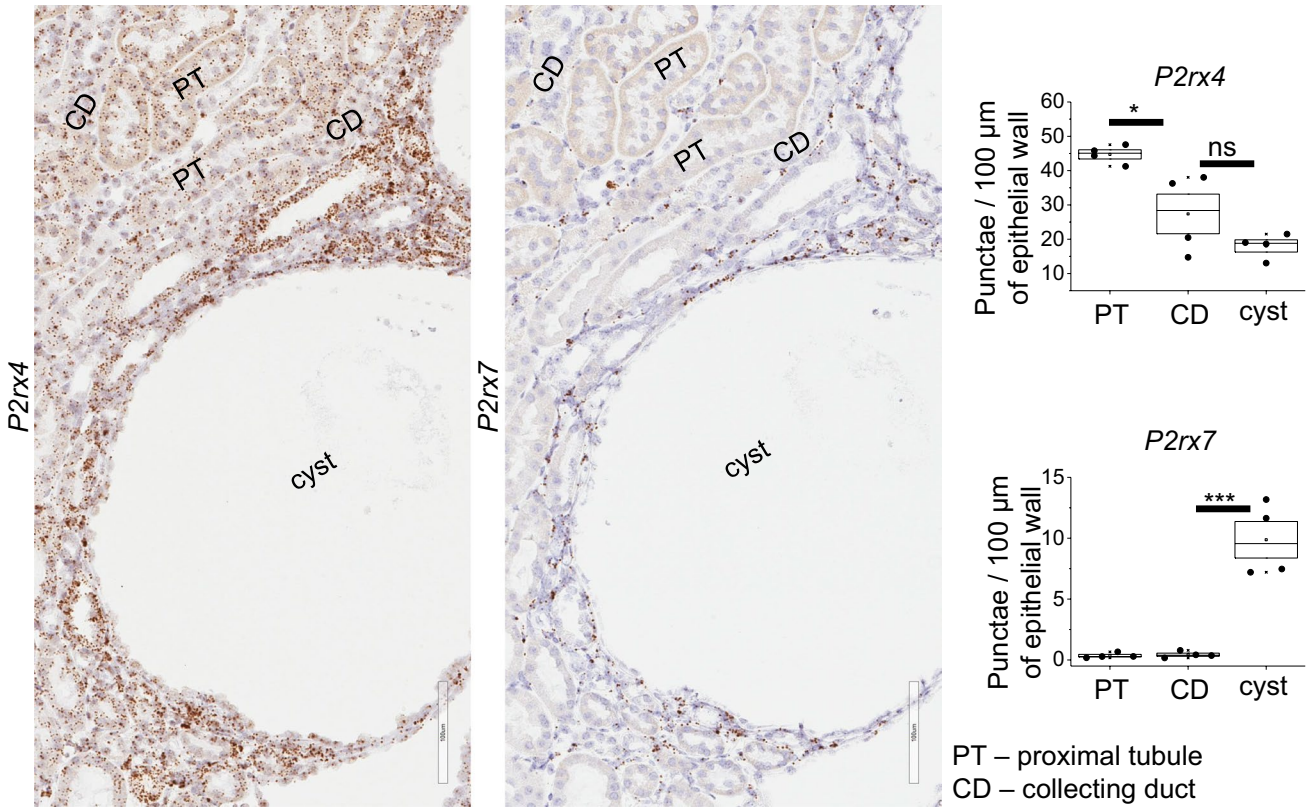

Fig. 3 Detection of *P2rX7* in cystic epithelium and normal tissues with in-situ hybridization. Expression of *P2rX4* and *P2rX7* was probed on consecutive histological slices with RNAscope in *Pkd1*$^{RC/RC}$ mouse kidneys. Brown punctae indicate mRNA presence in proximal tubules (PT), collecting ducts (CD), or cysts. Summary graphs on the right panel present signal intensity quantified as number of punctae per 100 µm of epithelial wall in the corresponding structures. *$p < 0.05$, ***$p < 0.001$ vs collecting ducts, Shapiro–Wilk (passed) and Dunnett test. ns—non-significant. Scale bar – 100 µm

presence of 10 µM forskolin, they form cyst-like spheroids if grown in Matrigel. Confocal microscopy on Fig. 7A demonstrates that the mpkCCD$_{cl4}$ spheroids express pannexin-1 in the lateral and basal plasma membrane with intensive phalloidin (actin cytoskeleton) overlapping on the luminal side. Pannexin-1 distribution in MDCK cells was described earlier by Shum and colleagues, who found that the protein does not express in plated cells but, if they are grown as monolayers on permeable supports or as cyst spheroids, resides on the apical side with a lower presence in the basolateral membrane [53]. Treatment with SIL14 lowers cysts' size both in mpkCCD$_{cl4}$ (Fig. 7B, C) and MDCK (Fig. 7D, E) cell 3D culture. We conclude that inhibition of pannexin-1 permeability with SIL14 precludes cyst development.

Discussion

ADPKD is a widespread disorder affecting a population with ~ 1:1,200 incidence worldwide [54, 55]. The only FDA-approved specific ADPKD treatment is tolvaptan, a vasopressin receptor antagonist, which reduces cellular cAMP levels, cannot fully stop or reverse disease progression, and has strong side effects (polyuria and thirst) [1]. Searching for new therapeutic targets remains the highest priority for ADPKD drug discovery. We and others explored the therapeutic potential of pannexin-1 targeting due to its specific upregulation in the cystic wall [14, 56, 57]. Attempts to inhibit pannexin-1 with brilliant blue-FCF and probenecid had beneficial effects in zebrafish and murine models of ADPKD [13, 56] indicating a promising direction. Here we tested the recently designed selective pannexin-1 blocker, SIL14, and confirmed its anti-cystic properties based on low dose effects on pannexin-1 in cell culture. These data provide a rationale for further testing SIL14 with *in-vivo* models of PKD.

Cyst formation is a complex process involving multiple aspects of cellular physiology. Transcriptomics on tissues isolated from the same organs reveals an altered expression of ~ 5 thousand genes in formed cysts in comparison to the collecting ducts not affected by cystogenesis. For comparison, all renal tissues of Spontaneously Hypertensive Rats show 383 differentially expressed genes vs control Wistar Kyoto strain [58]; in such a heterogenic structure as

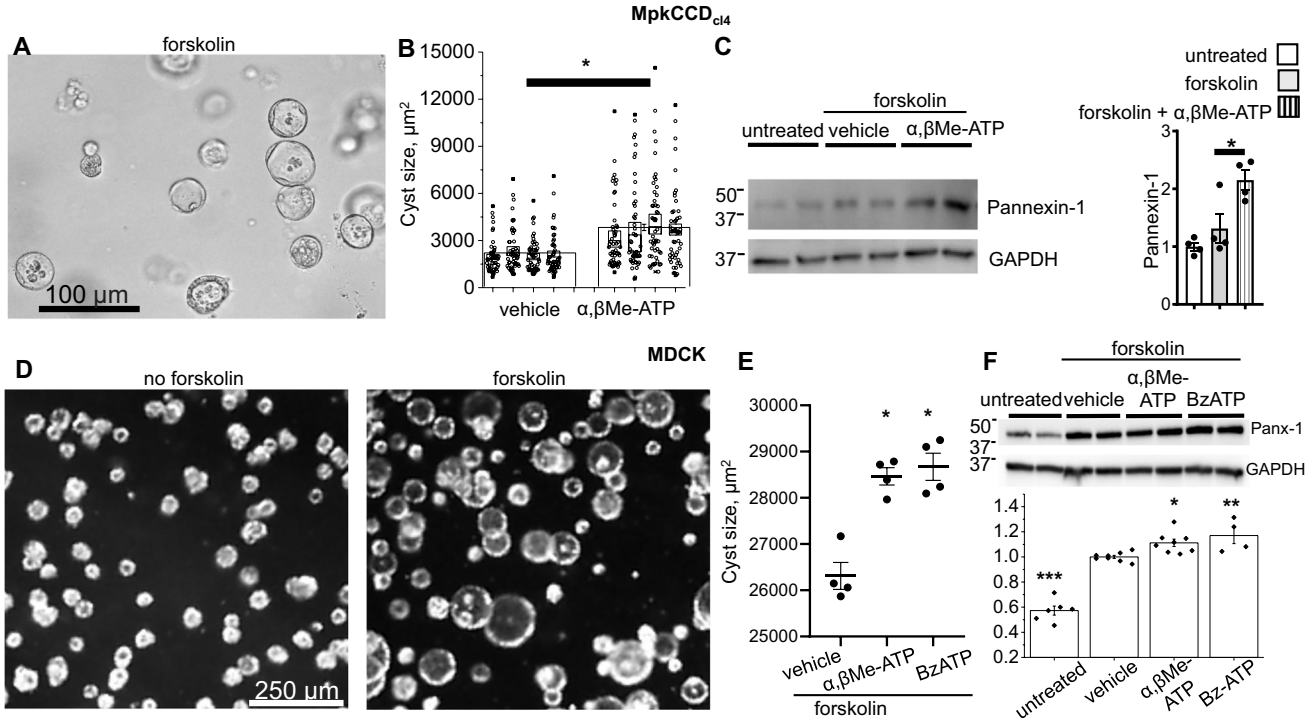

Fig. 4 Effect of P2X7 receptors stimulation on cyst growth in 3D cell culture. **A** Representative image of cysts formed by mpkCCD$_{cl4}$ cells in the presence of 10 μM forskolin. **B** Treatment with α,βMe-ATP (P2X agonist) increases the size of cysts grown from mpkCCD$_{cl4}$ cells. **C** Western blot analysis of pannexin-1 abundance in untreated (no forskolin in Matrigel), and vehicle or α,βMe-ATP treated groups in the presence of forskolin. Summary graphs on the right panels denote that stimulation with α,βMe-ATP increases pannexin-1 abundance. $N=4$ wells in each group, $n=50$ cysts in each well. **D** Representative images of MDCK cells grown in Matrigel in the absence (*left*) or presence (*right*) of 10 μM forskolin. Treatment of MDCK cysts with 100 μM α,βMe-ATP or 50 μM BzATP aggravates cystogenesis ($n=128$–232 cysts/well) (**E**) and increases the abundance of pannexin-1 (**F**). $^*p<0.05$; $^{**}p<0.01$; $^{***}p<0.001$ vs forskolin + vehicle; Shapiro–Wilk (passed) Dunnett test

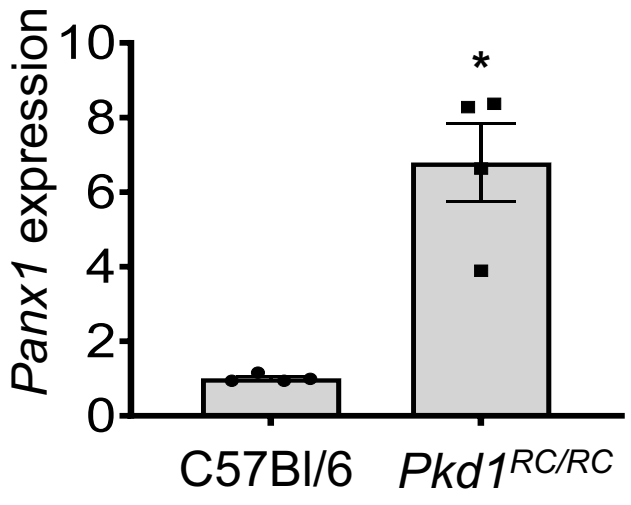

Fig. 5 Real-time PCR of *Panx1* mRNA level in the renal tissues of normal C57Bl/6 vs *Pkd1*$^{RC/RC}$ mice. Shapiro–Wilk (passed), unpaired *t*-test

glomeruli, 2719 differentially expressed genes were detected as a result of streptozotocin-induced diabetic kidney disease [59]. RNA sequencing was a convenient method to detect potential partners regulating pannexin-1. We focused on purinergic receptors because the P2X subfamily modulates pannexin-1 activity. Also, we earlier demonstrated with calcium imaging that cyst development in the autosomal recessive form of PKD is accompanied by abnormal expression of P2 receptors. In PCK rats, carrying the Pkhd1 mutation, the P2Y-mediated response to ATP was significantly reduced whereas P2X receptors took their place [12]. As metabotropic P2Y2 and P2Y4 are the most prevalent P2 species in normal collecting ducts [60–62] we suggested that the discovered re-profiling of cystic epithelia towards prevalence of ionotropic P2X receptors (evolutionary lower) reflects a deep tissue alteration.

In the present study, a similar process was detected in the cysts driven by the *Pkd1*$^{RC/RC}$ mutation. Loss of P2Y2 and P2Y4 was "compensated" by increased expression of P2X5 and P2X7 receptors. Although the role of P2X5 receptors in the *Pkd1*$^{RC/RC}$ mouse model is possible, we focused on P2X7 because the *P2rx5* gene is truncated and

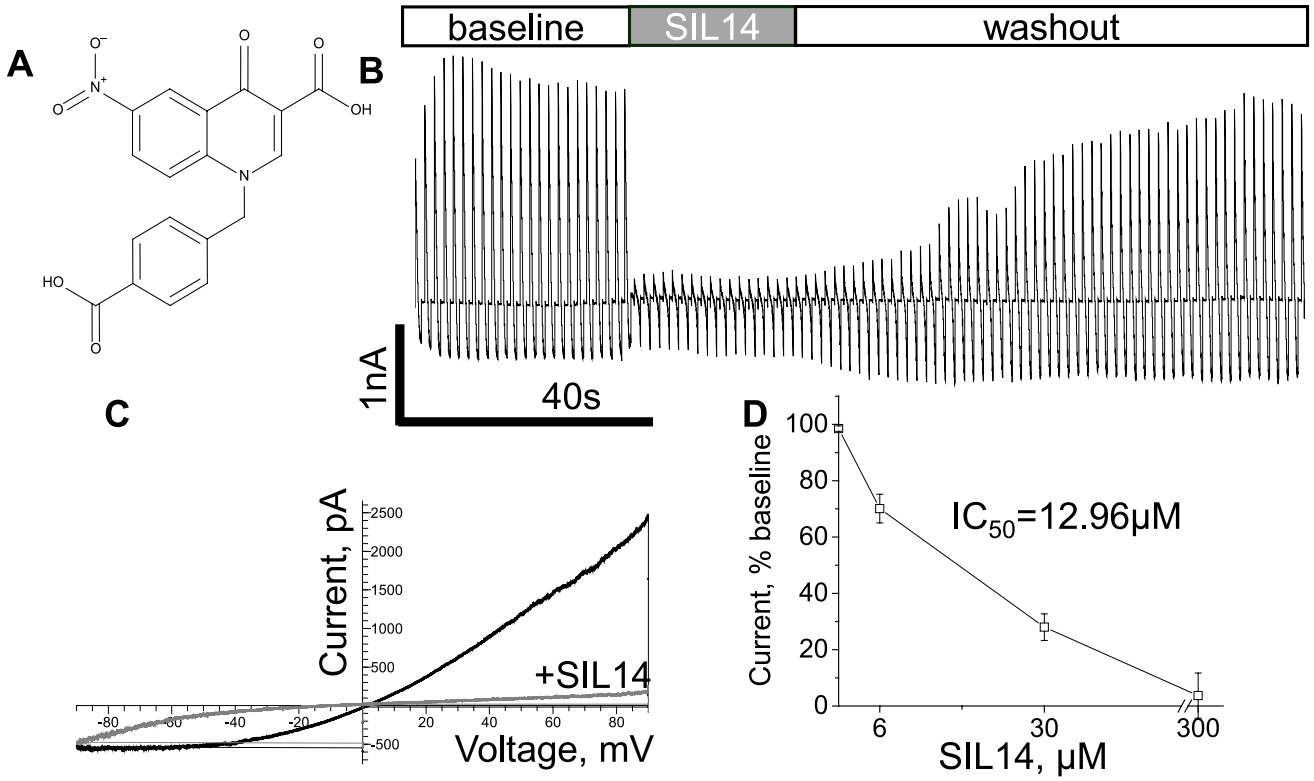

Fig. 6 Testing inhibitory properties of SIL14 with patch-clamp. **A** Chemical structure of SIL14. **B** Representative current trace of pannexin-1 activity with 300 μM SIL14 application. Whole-cell recordings were obtained on CHO cells transiently transfected with mPanx1 under [90; −90] mV ramps. **C** Current–voltage characteristic of pannexin-1 conductance before and after SIL14 application. **D** Dose dependency of SIL14 effect on pannexin-1 measured at + 80 mV reveals $IC_{50} = 12.96$ μM according to nonlinear regression analysis

non-functional in most of humans [63, 64], de-prioritizing the translational potential of the P2X5 direction. In contrast, P2X7 shows a panel of interesting properties for interventions. In contrast to *P2rx4*, which is ubiquitous in all renal tissues, *P2rX7* is expressed mainly in the cystic epithelium and pericystic tissue (Figs. 2and 3). This may explain the lack of effect of P2X4 modulation by ivermectin and 5-BDBD on the development of ARPKD in PCK rats [65]. The specific upregulation of both P2X7 and pannexin-1 in the cyst wall seems to have a dramatic effect due to the capability of P2X7 to regulate pannexin-1. For instance, stimulation of P2X receptors increases the abundance of pannexin-1 cyst size in Matrigel (Fig. 4). A similar effect was found earlier in a reverse *in-vivo* experiment involving *P2rx7* knockout in PCK rats: their kidneys had lower cyst size and less pannexin-1 protein, as shown by Western blot [66]. These observations are in accordance with reports showing that pannexin-1 is normally not abundant in healthy tubules, except for specific areas such as the macula densa, but is expressed in pathologic conditions such as acute kidney injury or cystogenesis [67, 68]. Functionally, P2X7-dependent pannexin-1 regulation can be illustrated by smaller cyst size in *P2rx7* deficient PCK rats and lower urinary ATP level than in normal PCK littermates [66].

In this work, we mainly focused on purinergic signaling, and some of the molecules we found to be differentially expressed could be particularly interesting in this key. For instance, one of the strongly upregulated molecules in our data is Anoctamin-6, a non-selective cation channel TMEM16F [69]. It belongs to the family of Ca^{+}-dependent ion channels and lipid scramblases [70]. One of its family members, Anoctamin-1, was shown to be upregulated in PKD cysts, and inhibition of its activity attenuated cyst growth through secretory effects [71–73]. Buchholz et.al. [72] also pointed out a possible regulation of Anoctamin-1 by purinergic signaling [74]. Given Anoctamin-6 protein and family properties, it could be a potential target for future studies.

Among significantly downregulated genes, we observed a lower expression of Transient Receptor Potential cation channel subfamily M Member 4 (TRPM4), another Ca^{+}-dependent cation channel [75]. It was previously linked to cilia maintenance [76, 77] and, giving a possible regulation of this channel by purinergic signaling [78], it could also be interesting to investigate further.

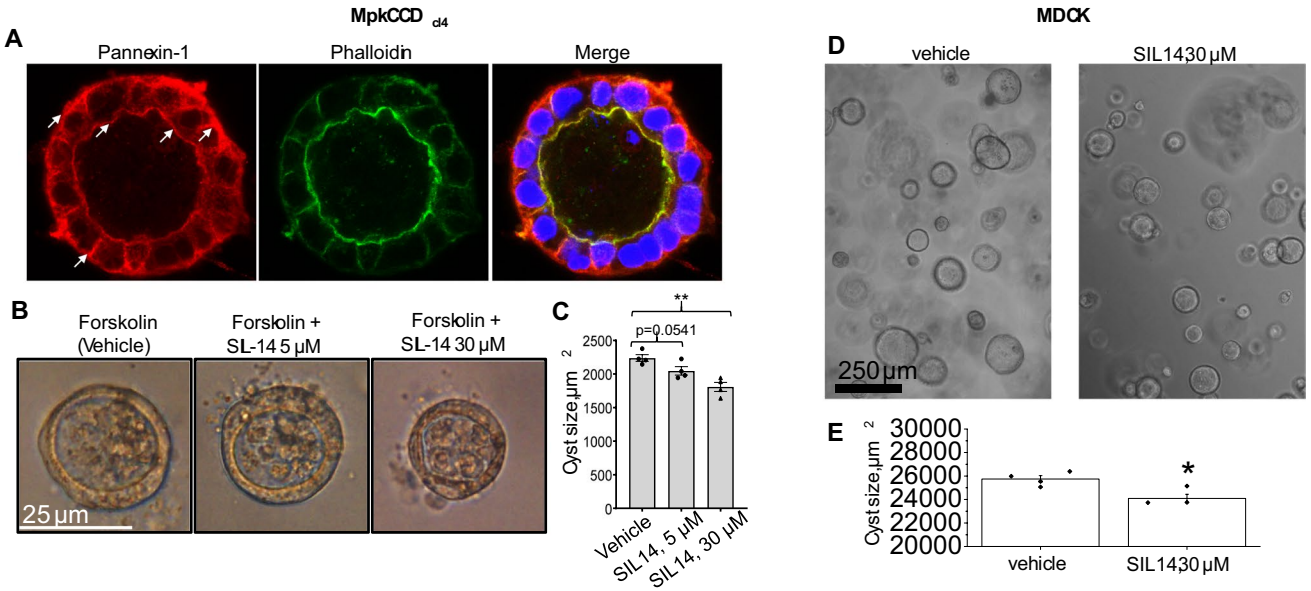

Fig. 7 Effect of SIL14 treatment on cyst growth in 3D cell culture. $MpkCCD_{cl4}$ or MDCK cells were grown in Matrigel in the presence of 10 µM forskolin. **A** Confocal microscopy shows the distribution of pannexin-1 and phalloidin in the plasma membrane of the $mpkCCD_{cl4}$ cyst epithelium. **B**, **C** Treatment with SIL14 reduces $mpkCCD_{cl4}$ cyst size. $n=4$ wells, $n=112$–150 cysts/well. $^{**}p<0.01$ vs vehicle, Shapiro–Wilk (passed), Dunnett test. **D** Representative image of cysts formed by MDCK cells in the presence of 30 µM SIL14. (**E**) Summary graph demonstrates that SIL14 reduces cyst size in comparison to the vehicle-treated group. $N=4$ wells, $n=90$–150 cysts/well. $^{*}p<0.05$ unpaired *t*-test

RNA-sequencing also gave us insights about other possible molecular targets in cystic epithelia. For instance, we identified strong upregulation of Thyroid Stimulating Hormone Receptor (TSHR) with downregulation of Thyroid Hormone Receptor alpha (Thra). This direction of future investigation could be particularly interesting, given that recent study implies a role of thyroid hormones in the progression of ADPKD [79].

We also observed a significant downregulation of Notch1 and Notch2. Both were linked to normal cilia development [80] and both upregulation and downregulation of the Notch signaling induce cystic phenotype in the kidney in different segments of the nephron [81–83]. Previous publications also pointed out the importance of the Notch signaling for collecting duct maintenance and cell fate [84]. A proximity assay reports interaction between Notch2 and pannexin-1 [85]. Given that our approach was mostly focused on comparing morphologically intact collecting ducts with cystic epithelia, we find this expression data especially interesting in the sense of the cyst heterogeneity.

Great amount of data supports a central role of cAMP in ADPKD [86]. Our RNA-seq data showed upregulation of ADCY7 (Adenylate cyclase 7) and downregulation of ADCY5 and ADCY6. Previous reports show that both ADCY5 and ADCY6 deficiency reduces cyst size in animal models [47, 87]. Decreased expression of ADCY5 and ADCY6 in cystic epithelia in our case could be due to higher basal expression of these adenylate cyclases in collecting ducts. We also used a different model of ADPKD–hypomorphic mutation of PKD1, unlike deletion of PKD1 or PKD2. This dosage of functional PKD1 and/or advanced age of our experimental mouse (22 months) could also explain downregulation of ADCY5 and ADCY6, as well as the possible existence of negative-feedback loop regulation of ADCY expression by cAMP levels. Upregulation of ADCY7 in a cystic model also has been shown previously [88], and it is possible that ADCY7 could be a primary source of cAMP in cystic epithelia in our ADPKD model. However, additional effort is required to perform RNA sequencing on younger RC mice to determine age dependency in transcriptome shift and delineate cause-effect relationships between the differentially expressed genes.

We also observed a differential expression of A-kinase anchoring proteins (AKAPs)—downregulation of AKAP8, and upregulation of AKAP9 and AKAP12 as well as upregulation of protein kinase A (PKA) subunits PRKAR1B and PRKAR2A. Collectively, this data shows upregulation of the cAMP-dependent pathway in cystic epithelia of our ADPKD model, as AKAPs' proteins can scaffold PKA [89]—a main biological effector of cAMP, to its respective targets. Interestingly, recent reports also suggest a purinergic-dependent activation of a similar pathway in the vascular cells where pannexin-1 is found in complex with AKAP5 and adenylate cyclase 5, increasing extracellular ATP release [90, 91].

Further investigation is necessary to clarify the role of specific family members of this pathway in ADPKD.

Study limitations Further development of the presented findings is required in different directions. The RNA sequencing was performed on large cysts isolated from mature females, and comparison on both sexes at different ages should be done to characterize transcriptome changes in a dynamic manner. Both aggravation and suppression of cystogenesis by targeting the pannexin-1/P2X7 pathway have modest but consistent [13, 31, 66] effect indicating that pannexin-1 is one of the contributors to cyst formation.

Supplementary Information The online version contains supplementary material available at https://doi.org/10.1007/s11302-025-10127-1.

Acknowledgements We thank the Henry Ford Hospital Histology Core for assistance with RNAScope and lectin staining.

Author contribution All experiments and analyses, drafting manuscript, research design and interpretation (V.I.); RNAseq informatics (A.W., Z.M., I.A., P.A.O.); RNAseq processing (P.S-M.); SIL14 production (L.C. and G.G.); multi-photon microscopy (T-D.L., P.A.O); patch-clamp, tissue isolation for RNAseq, research design, analyses, manuscript writing (T.S.P.). All authors have read and contributed to final version of the manuscript. Foreign in-kind contributions included sharing SIL14 by L.C. and G.G.

Funding This research is made possible by funding from NIH DK123266 (T.S.P) and DK131114 (P.A.O).

Data availability No datasets were generated or analysed during the current study.

Declarations

Conflicts of interests Tengis Pavlov provides consulting to SonoThera, Inc with a scope outside the submitted work. None of the other authors has any conflicts of interest, financial or otherwise, to disclose.

References

1. Gittus M, Haley H, Harris T et al (2025) Commentary: tolvaptan for autosomal dominant polycystic kidney disease (ADPKD) - an update. BMC Nephrol 26(1):79. https://doi.org/10.1186/s12882-025-03960-4
2. Guay-Woodford LM, Desmond RA (2003) Autosomal recessive polycystic kidney disease: the clinical experience in North America. Pediatrics 111(5):1072–1080
3. Kunnen SJ, Malas TB, Formica C, Leonhard WN, 't Hoen PAC, Peters DJM (2018) Comparative transcriptomics of shear stress treated Pkd1−/− cells and pre-cystic kidneys reveals pathways involved in early polycystic kidney disease. Biomed Pharmacother 108:1123–1134. https://doi.org/10.1016/j.biopha.2018.07.178
4. Song X, Di Giovanni V, He N et al (2009) Systems biology of autosomal dominant polycystic kidney disease (ADPKD): computational identification of gene expression pathways and integrated regulatory networks. Hum Mol Genet 18(13):2328–2343. https://doi.org/10.1093/hmg/ddp165
5. Menezes LF, Zhou F, Patterson AD et al (2012) Network analysis of a *Pkd1*-mouse model of autosomal dominant polycystic kidney disease identifies HNF4α as a disease modifier. PLoS Genet 8(11):e1003053. https://doi.org/10.1371/journal.pgen.1003053
6. Chen W-C, Tzeng Y-S, Li H (2008) Gene expression in early and progression phases of autosomal dominant polycystic kidney disease. BMC Res Notes 1(1):131. https://doi.org/10.1186/1756-0500-1-131
7. Friedrich S, Müller H, Riesterer C et al (2021) Identification of pathological transcription in autosomal dominant polycystic kidney disease epithelia. Sci Rep 11(1):15139. https://doi.org/10.1038/s41598-021-94442-8
8. Wildman SSP, Marks J, Turner CM et al (2008) Sodium-dependent regulation of renal amiloride-sensitive currents by apical P2 receptors. J Am Soc Nephrol 2008(4):731–742. https://doi.org/10.1681/asn.2007040443
9. Pochynyuk O, Rieg T, Bugaj V, Schroth J, Fridman A, Boss GR, Insel PA, Stockand JD, Vallon V (2010) Dietary Na+ inhibits the open probability of the epithelial sodium channel in the kidney by enhancing apical P2Y2-receptor tone. FASEB J. 24(6):2056–65. https://doi.org/10.1096/fj.09-151506
10. Grantham JJ, Mulamalla S, Swenson-Fields KI (2011) Why kidneys fail in autosomal dominant polycystic kidney disease. Nat Rev Nephrol 7(10):556–566. https://doi.org/10.1038/nrneph.2011.109
11. Wilson PD, Hovater JS, Casey CC, Fortenberry JA, Schwiebert EM (1999) ATP release mechanisms in primary cultures of epithelia derived from the cysts of polycystic kidneys. J Am Soc Nephrol 10(2):218–29
12. Palygin O, Ilatovskaya DV, Levchenko V et al (2018) Characterization of purinergic receptor expression in ARPKD cystic epithelia. Purinergic Signal. https://doi.org/10.1007/s11302-018-9632-5
13. Arkhipov SN, Potter DAL, Sultanova RF, Ilatovskaya DV, Harris PC, Pavlov TS (2023) Probenecid slows disease progression in a murine model of autosomal dominant polycystic kidney disease. Physiol Rep 11(7):e15652. https://doi.org/10.14814/phy2.15652
14. Arkhipov SN, Pavlov TS (2019) ATP release into ADPKD cysts via pannexin-1/P2X7 channels decreases ENaC activity. Biochem Biophys Res Commun 513(1):166–171. https://doi.org/10.1016/j.bbrc.2019.03.177

15. Crocetti L, Giovannoni MP, Guerrini G et al (2023) Design, synthesis and pharmacological evaluation of new quinoline-based Panx-1 channel blockers. Int J Mol Sci. https://doi.org/10.3390/ijms24032022
16. Hopp K, Ward CJ, Hommerding CJ et al (2012) Functional polycystin-1 dosage governs autosomal dominant polycystic kidney disease severity. J Clin Invest 122(11):4257–4273. https://doi.org/10.1172/JCI64313
17. Pavlov TS, Ilatovskaya DV, Palygin O, Levchenko V, Pochynyuk O, Staruschenko A (2015) Implementing patch clamp and live fluorescence microscopy to monitor functional properties of freshly isolated PKD epithelium. J Visualized Exp: Jove 103:e53035. https://doi.org/10.3791/53035
18. Pavlov TS, Ilatovskaya DV, Levchenko V, Li L, Ecelbarger CM, Staruschenko A (2013) Regulation of ENaC in mice lacking renal insulin receptors in the collecting duct. FASEB J 27(7):2723–2732. https://doi.org/10.1096/fj.12-223792
19. Umanath K, She R, Hassett C et al (2023) Urine cell transcriptomes implicate specific renal inflammatory pathways associated with difficult-to-control hypertension. J Am Heart Assoc 12(6):e026242. https://doi.org/10.1161/JAHA.122.026242
20. Amberger JS, Bocchini CA, Schiettecatte F, Scott AF, Hamosh A (2015) OMIM.org: online mendelian inheritance in man (OMIM®), an online catalog of human genes and genetic disorders. Nucleic Acids Res 43:D789–D798. https://doi.org/10.1093/nar/gku1205
21. Cerezo M, Sollis E, Ji Y et al (2024) The NHGRI-EBI gwas catalog: standards for reusability, sustainability and diversity. Nucleic Acids Res 53(D1):D998–D1005. https://doi.org/10.1093/nar/gkae1070
22. van Dam TJP, Kennedy J, van der Lee R et al (2019) CiliaCarta: an integrated and validated compendium of ciliary genes. PLoS One 14(5):e0216705. https://doi.org/10.1371/journal.pone.0216705
23. Ehrhart F, Willighagen E, Weitz E, Iyer A. Purinergic signaling (WP4900). https://www.wikipathways.org/instance/WP4900. Accessed 7 Jan 2026
24. Mouse Genome Database (MGD). http://www.informatics.jax.org. Accessed 7 Jan 2026
25. Baldarelli RM, Smith CL, Ringwald M, Richardson JE, Bult CJ, Group MGI (2024) Mouse Genome Informatics: an integrated knowledgebase system for the laboratory mouse. Genetics227(1) . https://doi.org/10.1093/genetics/iyae031
26. Shannon P, Markiel A, Ozier O et al (2003) Cytoscape: a software environment for integrated models of biomolecular interaction networks. Genome Res 13(11):2498–2504. https://doi.org/10.1101/gr.1239303
27. Bens M, Vallet V, Cluzeaud F et al (1999) Corticosteroid-dependent sodium transport in a novel immortalized mouse collecting duct principal cell line. J Am Soc Nephrol 10(5):923–934
28. Ho P-Y, Li H, Pavlov TS et al (2018) β1pix exchange factor stabilizes the ubiquitin ligase Nedd4-2 and plays a critical role in ENaC regulation by AMPK in kidney epithelial cells. J Biol Chem 293(29):11612–11624. https://doi.org/10.1074/jbc.RA118.003082
29. Mangoo-Karim R, Uchic M, Lechene C, Grantham JJ (1989) Renal epithelial cyst formation and enlargement in vitro: dependence on cAMP. Proc Natl Acad Sci U S A 86(15):6007–6011. https://doi.org/10.1073/pnas.86.15.6007
30. Molica F, Meens MJ, Dubrot J et al (2017) Pannexin1 links lymphatic function to lipid metabolism and atherosclerosis. Sci Rep 7(1):13706. https://doi.org/10.1038/s41598-017-14130-4
31. Crocetti L, Giovannoni MP, Pavlov TS, Ivanov V, Melani F, Guerrini G (2025) Synthesis of 3-carboxy-6-sulfamoylquinolones and mefloquine-based compounds as Panx1 blockers: molecular docking, electrophysiological and cell culture studies. Molecules 30(10):2171
32. Hopp K, Hommerding CJ, Wang X, Ye H, Harris PC, Torres VE (2015) Tolvaptan plus Pasireotide shows enhanced efficacy in a *PKD1* model. J Am Soc Nephrol 26(1):39–47. https://doi.org/10.1681/asn.2013121312
33. Agrawal A, Balcı H, Hanspers K et al (2023) WikiPathways 2024: next generation pathway database. Nucleic Acids Res 52(D1):D679–D689. https://doi.org/10.1093/nar/gkad960
34. Baldarelli RM, Smith CL, Ringwald M, Richardson JE, Bult CJ (2024) Mouse Genome Informatics: an integrated knowledgebase system for the laboratory mouse. Genetics. https://doi.org/10.1093/genetics/iyae031
35. Shibazaki S, Yu Z, Nishio S et al (2008) Cyst formation and activation of the extracellular regulated kinase pathway after kidney specific inactivation of *Pkd1*. Hum Mol Genet 17(11):1505–1516. https://doi.org/10.1093/hmg/ddn039
36. Fragiadaki M, Macleod FM, Ong ACM (2020) The controversial role of fibrosis in autosomal dominant polycystic kidney disease. Int J Mol Sci. https://doi.org/10.3390/ijms21238936
37. Kim D, Woo Y, Lee S et al (2018) Impact of miR-192 and miR-194 on cyst enlargement through EMT in autosomal dominant polycystic kidney disease. FASEB J 33:fj.201800563RR. https://doi.org/10.1096/fj.201800563RR
38. Streets A, Prosseda PP, Ong A (2020) Polycystin-1 regulates ARHGAP35-dependent centrosomal RhoA activation and ROCK signaling. JCI Insight 5(16):e135385. https://doi.org/10.1172/jci.insight.135385
39. Woo Y, Kim D, Koo N et al (2017) Profiling of miRNAs and target genes related to cystogenesis in ADPKD mouse models. Sci Rep. https://doi.org/10.1038/s41598-017-14083-8
40. Garcia-Mata R, Boulter E, Burridge K (2011) The "invisible hand": regulation of RHO GTPases by RHOGDIs. Nat Rev Mol Cell Biol 12(8):493–504. https://doi.org/10.1038/nrm3153
41. Møller L, Klip A, Sylow L (2019) Rho GTPases—emerging regulators of glucose homeostasis and metabolic health. Cells 8(5):434. https://doi.org/10.3390/cells8050434
42. Zou H, Shan C, Ma L, Liu J, Yang N, Zhao J (2020) Polarity and epithelial-mesenchymal transition of retinal pigment epithelial cells in proliferative vitreoretinopathy. PeerJ 8:e10136. https://doi.org/10.7717/peerj.10136
43. Patel S, Tang J, Overstreet JM et al (2019) Rac-GTPase promotes fibrotic TGF-β1 signaling and chronic kidney disease via EGFR, p53, and Hippo/YAP/TAZ pathways. FASEB J 33(9):9797–9810. https://doi.org/10.1096/fj.201802489RR
44. Liu Y, Suzuki YJ, Day RM, Fanburg BL (2004) Rho kinase–induced nuclear translocation of ERK1/ERK2 in smooth muscle cell mitogenesis caused by serotonin. Circ Res 95(6):579–586. https://doi.org/10.1161/01.RES.0000141428.53262.a4
45. Nagase M, Fujita T (2013) Role of Rac1–mineralocorticoid-receptor signalling in renal and cardiac disease. Nat Rev Nephrol 9(2):86–98. https://doi.org/10.1038/nrneph.2012.282
46. Hwang SH, Choi K, Badgandi H, White K, Xun Y, Qian F, Mukhopadhyay S (2025) Kidney cystogenesis in embryonic-and adult-onset ADPKD is suppressed from lack of adenylyl cyclase targeting to cilia. bioRxiv. https://doi.org/10.1101/2025.05.27.656198
47. Wang Q, Cobo-Stark P, Patel V, Somlo S, Han PL, Igarashi P (2018) Adenylyl cyclase 5 deficiency reduces renal cyclic AMP and cyst growth in an orthologous mouse model of polycystic kidney disease. Kidney Int 93(2):403–415. https://doi.org/10.1016/j.kint.2017.08.005
48. Praetorius HA, Leipziger J (2010) Intrarenal purinergic signaling in the control of renal tubular transport. Annu Rev Physiol 72:377–393. Not in File
49. Sáez PJ, Vargas P, Shoji KF, Harcha PA, Lennon-Duménil A-M, Sáez JC (2017) ATP promotes the fast migration of dendritic cells through the activity of pannexin 1 channels and P2X7 receptors. Sci Signal 10(506):eaah7107. https://doi.org/10.1126/scisignal.aah7107

50. Draganov D, Gopalakrishna-Pillai S, Chen YR et al (2015) Modulation of P2X4/P2X7/Pannexin-1 sensitivity to extracellular ATP via ivermectin induces a non-apoptotic and inflammatory form of cancer cell death. Sci Rep 5(1):16222. https://doi.org/10.1038/srep16222
51. Outeda P, Menezes L, Hartung EA et al (2017) A novel model of autosomal recessive polycystic kidney questions the role of the fibrocystin C-terminus in disease mechanism. Kidney Int 92(5):1130–1144. https://doi.org/10.1016/j.kint.2017.04.027
52. Lohman AW, Weaver JL, Billaud M et al (2012) S-nitrosylation inhibits pannexin 1 channel function. J Biol Chem 287(47):39602–39612. https://doi.org/10.1074/jbc.M112.397976
53. Shum MG, Shao Q, Lajoie P, Laird DW (2019) Destination and consequences of Panx1 and mutant expression in polarized MDCK cells. Exp Cell Res 381(2):235–247. https://doi.org/10.1016/j.yexcr.2019.05.016
54. Xue C, Zhou C-C, Wu M, Mei C-L (2016) The clinical manifestation and management of autosomal dominant polycystic kidney disease in China. Kidney Dis 2(3):111–119. https://doi.org/10.1159/000449030
55. Torres VE, Ahn C, Barten TRM et al (2025) KDIGO 2025 clinical practice guideline for the evaluation, management, and treatment of autosomal dominant polycystic kidney disease (ADPKD): executive summary. Kidney Int 107(2):234–254. https://doi.org/10.1016/j.kint.2024.07.010
56. Verschuren EHJ, Rigalli JP, Castenmiller C et al (2020) Pannexin-1 mediates fluid shear stress-sensitive purinergic signaling and cyst growth in polycystic kidney disease. FASEB J 34(5):6382–6398. https://doi.org/10.1096/fj.201902901R
57. van Megen WH, van Houtert TJ, Bos C, Peters DJM, de Baaij JHF, Hoenderop JGJ (2024) Inhibition of pannexin-1 does not restore electrolyte balance in precystic Pkd1 knockout mice. Physiol Rep 12(7):e15956. https://doi.org/10.14814/phy2.15956
58. Wei J, Tan F, Long X et al (2023) RNA-Seq transcriptome analysis of renal tissue from spontaneously hypertensive rats revealed renal protective effects of dapagliflozin, an inhibitor of sodium-glucose cotransporter 2. Eur J Pharm Sci 189:106531. https://doi.org/10.1016/j.ejps.2023.106531
59. Elzinga SE, Eid SA, McGregor BA et al (2023) Transcriptomic analysis of diabetic kidney disease and neuropathy in mouse models of type 1 and type 2 diabetes. Dis Models Mech 16(10).https://doi.org/10.1242/dmm.050080
60. Cuffe JE, Bielfeld-Ackermann A, Thomas J, Leipziger J, Korbmacher C (2000) ATP stimulates Cl− secretion and reduces amiloride-sensitive Na+ absorption in M-1 mouse cortical collecting duct cells. J Physiol 524(1):77–90. https://doi.org/10.1111/j.1469-7793.2000.00077.x
61. Turner CM, Vonend O, Chan C, Burnstock G, Unwin RJ (2003) The pattern of distribution of selected ATP-sensitive P2 receptor subtypes in normal rat kidney: an immunohistological study. Cells Tissues Organs 175(2):105–117. https://doi.org/10.1159/000073754
62. Bailey MA, Imbert-Teboul M, Turner C et al (2000) Axial distribution and characterization of basolateral P2Y receptors along the rat renal tubule. Kidney Int 58(5):1893–1901. https://doi.org/10.1111/j.1523-1755.2000.00361.x
63. Duckwitz W, Hausmann R, Aschrafi A, Schmalzing G (2006) P2X5 subunit assembly requires scaffolding by the second transmembrane domain and a conserved aspartate*. J Biol Chem 281(51):39561–39572. https://doi.org/10.1074/jbc.M606113200
64. King BF (2023) Rehabilitation of the P2X5 receptor: a re-evaluation of structure and function. Purinergic Signal 19(2):421–439. https://doi.org/10.1007/s11302-022-09903-0
65. Xu B, Nikolaienko O, Levchenko V et al (2022) Modulation of P2X4 receptor activity by ivermectin and 5-BDBD has no effect on the development of ARPKD in PCK rats. Physiol Rep 10(21):e15510. https://doi.org/10.14814/phy2.15510
66. Arkhipov SN, Potter DAL, Geurts AM, Pavlov TS (2019) Knockout of P2rx7 purinergic receptor attenuates cyst growth in a rat model of ARPKD. Am J Physiol Renal Physiol 317(6):F1649–F1655. https://doi.org/10.1152/ajprenal.00395.2019
67. DeLalio LJ, Masati E, Mendu S et al (2020) Pannexin 1 channels in renin-expressing cells influence renin secretion and blood pressure homeostasis. Kidney Int 98(3):630–644. https://doi.org/10.1016/j.kint.2020.04.041
68. Poudel N, Zheng S, Skrypnyk N et al (2025) Proximal tubule pannexin 1 contributes to mitochondrial dysfunction and cell death during acute kidney injury. Am J Physiol Renal Physiol. https://doi.org/10.1152/ajprenal.00226.2024
69. Reichhart N, Schöberl S, Keckeis S et al (2019) Anoctamin-4 is a bona fide Ca2+-dependent non-selective cation channel. Sci Rep 9(1):2257. https://doi.org/10.1038/s41598-018-37287-y
70. Kalienkova V, Clerico Mosina V, Paulino C (2021) The groovy TMEM16 family: molecular mechanisms of lipid scrambling and ion conduction. J Mol Biol 433(16):166941. https://doi.org/10.1016/j.jmb.2021.166941
71. Xu T, Chen M, Xu Q et al (2022) Anoctamin 1 inhibition suppresses cystogenesis by enhancing ciliogenesis and the ciliary dosage of polycystins. Front Biosci Landmark Ed 27(7):216. https://doi.org/10.31083/j.fbl2707216
72. Buchholz B, Faria D, Schley G, Schreiber R, Eckardt K-U, Kunzelmann K (2014) Anoctamin 1 induces calcium-activated chloride secretion and proliferation of renal cyst–forming epithelial cells. Kidney Int 85(5):1058–1067. https://doi.org/10.1038/ki.2013.418
73. Tanaka T, Nangaku M (2014) ANO1: an additional key player in cyst growth. Kidney Int 85(5):1007–1009. https://doi.org/10.1038/ki.2013.436
74. Cabrita I, Kraus A, Scholz JK et al (2020) Cyst growth in ADPKD is prevented by pharmacological and genetic inhibition of TMEM16A *in vivo*. Nat Commun 11(1):4320. https://doi.org/10.1038/s41467-020-18104-5
75. Guo J, She J, Zeng W, Chen Q, Bai XC, Jiang Y (2017) Structures of the calcium-activated, non-selective cation channel TRPM4. Nature 552(7684):205–209. https://doi.org/10.1038/nature24997
76. Flannery RJ, Kleene NK, Kleene SJ (2015) A TRPM4-dependent current in murine renal primary cilia. Am J Physiol Renal Physiol 309(8):F697-707. https://doi.org/10.1152/ajprenal.00294.2015
77. Kleene SJ (2024) Hyperosmolality activates polycystin-2 and TRPM4 in renal primary cilium. Pflügers Archiv - European Journal of Physiology. https://doi.org/10.1007/s00424-024-03050-8
78. Li Y, Baylie RL, Tavares MJ, Brayden JE (2014) TRPM4 channels couple purinergic receptor mechanoactivation and myogenic tone development in cerebral parenchymal arterioles. J Cereb Blood Flow Metab 34(10):1706–1714. https://doi.org/10.1038/jcbfm.2014.139
79. Lavecchia AM, Trillini M, Cerullo D et al (2024) #339 Thyroid hormone levels critically contribute to ADPKD progression. Nephrol Dial Transplant. https://doi.org/10.1093/ndt/gfae069.143
80. Mukherjee M, Ratnayake I, Janga M et al (2019) Notch signaling regulates Akap12 expression and primary cilia length during renal tubule morphogenesis. bioRxiv 760181. https://doi.org/10.1101/760181
81. Belyea BC, Xu F, Wiltsie M et al (2023) Overexpression of notch signaling in renin cells leads to a polycystic kidney phenotype. Clin Sci 137(1):35–45. https://doi.org/10.1042/cs20220496
82. Surendran K, Selassie M, Liapis H, Krigman H, Kopan R (2010) Reduced notch signaling leads to renal cysts and papillary microadenomas. J Am Soc Nephrol 21(5):819–832. https://doi.org/10.1681/asn.2009090925
83. Ren H, Mu C, Wang Y et al (2025) Notch2 inhibition and kidney cyst growth in autosomal dominant polycystic kidney disease. J Am Soc Nephrol. https://doi.org/10.1681/asn.0000000592

84. Mukherjee M, deRiso J, Otterpohl K et al (2019) Endogenous notch signaling in adult kidneys maintains segment-specific epithelial cell types of the distal tubules and collecting ducts to ensure water homeostasis. J Am Soc Nephrol 30(1):110–126. https://doi.org/10.1681/asn.2018040440
85. Go CD, Knight JDR, Rajasekharan A et al (2021) A proximity-dependent biotinylation map of a human cell. Nature 595(7865):120–124. https://doi.org/10.1038/s41586-021-03592-2
86. Zhou X, Torres VE (2022) Emerging therapies for autosomal dominant polycystic kidney disease with a focus on cAMP signaling. Front Mol Biosci 9:981963. https://doi.org/10.3389/fmolb.2022.981963
87. Rees S, Kittikulsuth W, Roos K, Strait KA, Van Hoek A, Kohan DE (2014) Adenylyl cyclase 6 deficiency ameliorates polycystic kidney disease. J Am Soc Nephrol 25(2):232–237. https://doi.org/10.1681/asn.2013010077
88. Pandey P, Qin S, Ho J, Zhou J, Kreidberg JA (2011) Systems biology approach to identify transcriptome reprogramming and candidate microRNA targets during the progression of polycystic kidney disease. BMC Syst Biol 5:56. https://doi.org/10.1186/1752-0509-5-56
89. Dessauer CW (2009) Adenylyl cyclase--A-kinase anchoring protein complexes: the next dimension in cAMP signaling. Mol Pharmacol 76(5):935–941. https://doi.org/10.1124/mol.109.059345
90. Martín-Aragón Baudel M, Flores-Tamez VA, Hong J et al (2022) Spatiotemporal control of vascular Ca(V)1.2 by α1(C) S1928 phosphorylation. Circ Res 131(12):1018–1033. https://doi.org/10.1161/circresaha.122.321479
91. Hong J, Martín-Aragón Baudel M, Niloy SI, Taylor J, Mohabbat Y, Moustafa Y, Pereira Da Silva E, O'Donnell BL, Zhu Z, Daghbouche-Rubio N, Reddy GR, Sasse KC, Ward SM, Xiang YK, Isakson BE, Nieves-Cintrón M, Navedo MF (2025) Arterial myocyte pannexin 1 channel controls vascular reactivity in diabetic hyperglycemia. Circ Res 137(5):646–663. https://doi.org/10.1161/CIRCRESAHA.125.326260

Veniamin Ivanov Currently, I'm a Postdoctoral Fellow at Henry Ford Health system, Department of Hypertension and Vascular Research. I received my PhD from Niigata University, Kidney Research Center, Molecular Biology division with focus on the podocytes. Current research is focused on Polycystic Kidney Decease and Hypertension, and I hope that our research will identify new mechanisms and offer better treatment options. My long-term goal is to become a physician scientist and apply acquired knowledge towards patient care.